Lattice dynamics in $Ba_xSr_{1-x}TiO_3$ single crystals: A Raman study

D. A. Tenne,[1,*] A. Soukiassian,[2] X. X. Xi,[1,2,3] H. Choosuwan,[3] R. Guo,[2,3] and A. S. Bhalla[2,3]
[1]*Department of Physics, The Pennsylvania State University, University Park, Pennsylvania 16802, USA*
[2]*Department of Materials Science and Engineering, The Pennsylvania State University, University Park, Pennsylvania 16802, USA*
[3]*Materials Research Institute, The Pennsylvania State University, University Park, Pennsylvania 16802, USA*
(Received 15 January 2004; revised manuscript received 9 August 2004; published 3 November 2004)

The lattice dynamical properties of $Ba_xSr_{1-x}TiO_3$ single crystals with $x=0.05$, 0.1, 0.2, 0.35, and 0.5 have been studied by Raman spectroscopy in the temperature range 5–300 K. We present the data on the composition and temperature dependence of the phonon modes in $Ba_xSr_{1-x}TiO_3$, in particular, the soft modes. At low temperatures, the well-defined E and A_1 soft modes have been observed in the crystals of all compositions studied. For low Ba content ($x<0.2$) the soft modes extrapolate to zero and remain underdamped in the entire temperature range, indicating the displacive type of the ferroelectric phase transition. For $x\gtrsim 0.2$, i.e., in the composition range of the $Ba_xSr_{1-x}TiO_3$ phase diagram where three ferroelectric phases exist, the soft modes exhibit less softening and become heavily damped in the temperature range corresponding to the orthorhombic and tetragonal phases. This demonstrates that the order-disorder-type behavior becomes stronger with increasing Ba content. However, no first-order Raman scattering in the cubic phase was observed in $Ba_xSr_{1-x}TiO_3$ of compositions studied, in contrast to pure $BaTiO_3$. The temperature behavior of the A_1 soft mode indicates that the ferroelectric phase transition is of the first order in $Ba_xSr_{1-x}TiO_3$ with $x\gtrsim 0.2$, and turns into the second order for smaller Ba concentrations.

DOI: 10.1103/PhysRevB.70.174302 PACS number(s): 63.70.+h, 77.84.Dy, 78.30.Er

I. INTRODUCTION

Barium strontium titanate $Ba_xSr_{1-x}TiO_3$ (BST) is a typical perovskite ferroelectric solid solution extensively studied for many years.[1,2] Recently, thin film BST has been the subject of many studies because of its potential for device applications, such as dynamic random access memory or tunable microwave devices.[3,4] An issue of major importance for device applications of ferroelectric materials is the understanding of the difference between thin film and bulk crystal behaviors. Because lattice dynamics is essential for understanding the fundamental properties of ferroelectrics, a knowledge of lattice dynamics in BST is indispensable for basic and applied research of this material. For ferroelectrics, the lowest frequency transverse optical phonon, the soft mode, is of particular importance. Its eigenfrequency approaches zero at a critical temperature T_c where a lattice instability leads to a ferroelectric phase transition. In the paraelectric phase, the zone-center optical phonons are connected to the static dielectric constant via the Lyddane-Sachs-Teller relation.[5] Lattice dynamics of bulk single crystal and polycrystalline $BaTiO_3$ (BTO)[6–13] and $SrTiO_3$ (STO)[14–16] have been investigated extensively using various experimental techniques including Raman scattering. In comparison, despite the large number of studies dealing with BST, the investigation of lattice dynamical properties in this widely used device material is very limited. It is very difficult to find a lattice dynamics reference of BST single crystals to assist the lattice dynamical studies of BST thin films. The present work attempts to change this situation by presenting a detailed Raman study of vibrational spectra of BST single crystals.

The pure compounds, $BaTiO_3$ and $SrTiO_3$, have the same cubic perovskite structure in the high-temperature phase. Barium titanate is a typical ferroelectric, which undergoes three consecutive phase transitions from a cubic $m3m$ to a tetragonal $4mm$ phase at 403 K, then to an orthorhombic $mm2$ phase at 278 K, and, finally, to a rhombohedral $3m$ phase at 183 K.[17] In $Ba_xSr_{1-x}TiO_3$ the temperatures of these three phase transitions decrease nearly linearly with decreasing x and coincide at about 100 K and $x\approx 0.15$.[18] For lower Ba concentrations only one ferroelectric phase exists. Bulk $SrTiO_3$ is an incipient ferroelectric (quantum paraelectric), in which the ferroelectric phase transition is suppressed by quantum fluctuations.[19] An antiferrodistortive cubic-tetragonal phase transition occurs at 105 K, which involves the rotation of the Ti-O octahedra. The tetragonal structure $4/mmm$ is still centrosymmetric and, hence, not ferroelectric.

The perovskite crystal structure has five atoms (one formula unit) per unit cell, therefore, there are 12 optical vibrational modes. In the cubic phase $m3m$ the zone-center optical phonons belong to $3F_{1u}+F_{2u}$ irreducible representations. Each of the F_u modes is triply degenerate, and all of them are of odd symmetry with respect to the inversion, therefore, Raman inactive. The F_{1u} modes are infrared active, while the F_{2u} modes are silent. Upon transition to the tetragonal phase $4mm$ the F_{1u} modes split into A_1 and E modes, and the F_{2u} phonon gives rise to B_1 and E modes. The E modes are doubly degenerate. In the orthorhombic phase $mm2$ the optical vibrations belong to A_1, A_2, B_1, and B_2 symmetry. In the lowest temperature, rhombohedral phase, the modes originating from the cubic F_{1u} phonons are split into A_1 and E modes, while the F_{2u} vibrations produce A_2 and E modes. The symmetric A_1 and E modes are Raman active. For the A_1 phonons the atomic displacements are parallel to the z axis (polar axis in the ferroelectric phases), while for the E modes atoms vibrate in the xy plane perpendicular to the polar axis. Also, in polar crystals, to which BST belongs, long-range electrostatic interaction results in additional splitting of each

optical phonon branch into transverse (TO) and longitudinal (LO) modes.

In BTO, the F_{1u} soft mode is heavily overdamped in the paraelectric cubic phase.[7–9] The term "overdamping" usually implies the ratio $\Gamma/\omega > \sqrt{2}$, where Γ is the phonon mode linewidth, and ω is the mode frequency. Upon this condition there is no distinct peak at finite frequency in Raman spectra. In the tetragonal phase of BTO, the soft mode splits into A_1 and E components, and the E soft mode remains overdamped. [7–9] In the orthorhombic phase, Laabidi *et al.*[20] reported the damping of the soft mode to decrease, so the mode becomes underdamped below 253 K. At the transition to the rhombohedral phase, according to Laabidi *et al.*[20] the soft mode abruptly stiffens up to $\sim 200\ \mathrm{cm}^{-1}$.

The heavy overdamping of the soft mode in BTO has been attributed to the order-disorder character of the ferroelectric phase transition in this material. For a long time since the discovery of ferroelectricity, barium titanate had been considered as an example of displacive ferroelectrics,[2] supported by earlier neutron,[21] Raman[7–9] and hyper-Raman[10] experiments, which demonstrated the existence of the soft TO phonon mode and its softening in the paraelectric phase with decreasing the temperature. However, the soft mode becomes highly overdamped near the Curie temperature, and its frequency does not extrapolate to zero at T_c. A discrepancy was observed near T_c between the dielectric constant obtained from capacitance measurements and from the soft mode frequencies via Lyddane-Sachs-Teller relation.

The order-disorder picture was initially suggested for $BaTiO_3$ in order to explain the observation of strong diffusive x-ray scattering.[22] It was later supported by the observation of the symmetry-forbidden first-order Raman lines above T_c, in the cubic phase, and by electronic paramagnetic resonance (EPR) studies.[23] An eight-site order-disorder model was proposed, in which the Ti ions in the paraelectric phase do not reside in the center of the cubic unit cell. Instead there are eight equivalent off-center energy minima located along [111] directions. In the high-temperature phase all sites are occupied by Ti ion with equal probability, and the average symmetry is cubic. Four sites become preferentially occupied in the tetragonal phase, only two nearest-neighbor sites are the most probably occupied in the orthorhombic phase, and only one site remains occupied in rhombohedral phase. The *ab initio* calculations of the total energy as a function of Ti ion displacements[24] in the cubic phase show the presence of absolute energy minima at the [111] off-center positions, while local (higher energy) minima exist for [100] displacements. The low-frequency ($\sim 10^8$ Hz) motion of Ti ion between equivalent off-center cites was suggested to be responsible for the discrepancy between the dielectric constant and soft mode behavior near the Curie temperature. This relaxational motion leads to the appearance of intensive low-frequency near-excitation scattering in Raman spectra (so-called central peak). The observation of a central peak in the Raman spectra of $BaTiO_3$[25,26] provided the evidence of such a slow relaxational motion. Later femtosecond time-resolved stimulated Raman measurements[27] allowed one to distinguish between overdamped soft modes and relaxational modes. Recent nuclear magnetic resonance studies[28] demonstrated the coexistence of both displacive and order-disorder components in the phase transition mechanism in BTO and the breakdown of local cubic symmetry due to the motion of Ti ions between off-center sites in the paraelectric phase.

Experimental results have established that phase transitions in BTO have both displacive and order-disorder-like properties. Theoretical models were developed[29–32] which describe the dynamics of ions as consisting of two components with different time scale: rapid vibrations associated with the soft phonons and slow relaxational modes. In intermediate ferroelectrics like $BaTiO_3$ there is strong coupling between the soft and relaxational modes, probably leading to overdamping of the soft mode. First-principles theory of ferroelectric phase transitions for $BaTiO_3$ (Ref. 33) also shows the phase transitions to be intermediate between order-disorder and displacive character.

In contrast to BTO, STO remains paraelectric down to low temperatures, the zone-center optical phonons remain Raman inactive. The spectrum of STO crystal is dominated by the second-order features. Application of an electric field breaks the inversion symmetry, thus allowing the observation of the soft mode by Raman scattering.[15] The soft mode is well defined and does not tend to zero as temperature decreases, saturating at ~ 32 K due to quantum fluctuations. The soft mode in STO exhibits no overdamping over the entire temperature range, and excellent agreement is observed between the dielectric constant and the soft mode, both in temperature and electric field dependence.[15] No significant disorder effects have been observed in STO, and therefore it is considered as predominantly displacive-type ferroelectric. Due to the antiferrodistortive phase transition at 105 K, sharp peaks of R modes, which are the zone-edge (R point) phonons, become Raman active via double folding of the Brillouin zone.[14]

Since the pure BTO and STO show different behavior, the properties of solid solution $Ba_xSr_{1-x}TiO_3$ can be expected to evolve with composition. The order-disorder behavior (such as overdamping) should be enhanced with increasing Ba contents. However, the experimental results of lattice dynamics in BST are very limited. So far, Lemanov[34] reported the most detailed Raman scattering result in BST. They measured at 6 K the concentration dependence of Raman lines in BST with $x=0$ to 1, mostly in ceramic samples. The low-temperature Raman lines were assigned to various phonon modes. No temperature dependence of the Raman spectra and phonon modes was reported in this work. A micro-Raman study of Dobal *et al.*[35] focused on the cubic-tetragonal phase transition temperature as a function of composition x in Ba-rich $Ba_xSr_{1-x}TiO_3$ ceramics ($x=0.65-1.0$). In another study,[36] Naik *et al.* reported Raman spectra of ceramic bulk and thin-film samples of polycrystalline BST with $x=0.7-1.0$ between room temperature and 350 °C. The loss of intensity of several tetragonal-phase phonon modes was used to determine the ferroelectric to paraelectric phase-transition temperatures. In these Ba-rich compositions, they observed broad first-order Raman features well beyond T_c, similar to the behavior of pure BTO. Kuo *et al.*[37] reported Raman and x-ray diffraction studies of polycrystalline BST samples in the entire composition range at room temperature.

At this temperature, they found that BST is ferroelectric for $x \geqslant 0.7$.

There have been several Raman studies of BST thin films, whose lattice dynamical properties are influenced by strain and defects in the films. By measuring the soft mode phonons in epitaxial BST films with $x=0.05$, 0.1, 0.2, 0.35, and 0.5, we found that the lattice dynamical behaviors in the films are strikingly similar to those in relaxor ferroelectrics, which was explained by the existence of polar nanoregions in the thin films.[38,39] Petzelt and Ostapchuk *et al.*[40] also pointed out an important difference in the soft mode behavior of BST thin films and ceramics, such as the soft mode hardening in thin films and presence of the symmetry-forbidden first-order Raman peaks in the spectra of paraelectric phase. They attributed these effects to polar grain boundaries, porosity and other structural distortions in films. Yuzyuk *et al.*[41] applied Raman spectroscopy to study Ba-rich ($x \geqslant 0.55$) $Ba_xSr_{1-x}TiO_3$ films grown on MgO substrates, focusing mainly on the strain effects on the ferroelectric phase transitions in films. They observed the soft phonon modes in the spectra of thin films and studied the influence of composition variation on the soft modes. Kim *et al.*[42] studied the effect of crystallinity on the microwave dielectric losses in BST films and found the correlation between the increased dielectric loss and the symmetry-breaking defects evidenced by Raman spectra.

Given the technological importance of the BST material, in both bulk and thin film forms, it is imperative to have a comprehensive understanding of its lattice dynamical properties, preferably measured using high quality single crystals which are free from extrinsic effects due to strain and defects as in thin films. The existing results in the literature, although very informative and important, have not provided such a comprehensive picture of lattice dynamics in BST. There is no lattice dynamics study based on BST single crystals. In this work we present a detailed Raman study of BST single crystals with different compositions and measured between 5–300 K. We found that for low Ba content ($x<0.2$) the soft modes extrapolate to zero at T_c and remain underdamped, indicating a displacive type of the ferroelectric phase transition. For $x \gtrsim 0.2$, the soft modes become heavily damped in the orthorhombic and tetragonal phases, and the order-disorder-type behavior becomes stronger with increasing Ba content. No first-order Raman scattering in the cubic phase of BST is observed for all compositions studied ($x \leqslant 0.5$), in contrast to pure BTO. These single crystal results can be used as a reference point for the understanding of the lattice dynamical properties in BST ceramics and thin films.

II. EXPERIMENTAL DETAILS

The lack of literature data on BST single crystals may be due to the difficulties in growing high purity crystals. The BST single crystals with $x=0.05$, 0.1, 0.2, 0.35, and 0.5 for this study were grown by laser-heated pedestal growth (LHPG) technique.[43] Dense ceramics of BST with homogenous microstructure and small grains were first prepared by the solid state reaction and cut into rods of 20 mm $\times$ 1 mm $\times$ 1 mm in size. During the growth, the laser radiation of a CO_2 laser (55 W maximum power) was focused to form a hot zone on the rod. The temperature of the hot zone was kept around the *liquidus* line temperature. The rod was moved slowly with respect to the molten zone at a pull rate adjusted according to the BST composition. The LHPG process produced BST crystals with 15 mm in length and 0.8 mm in diameter. X-ray diffraction showed single phase and from the Laue back reflection patterns the growth direction was identified as $\langle 110 \rangle$, the same as that of the seed crystal. The crystals studied in this work are $\sim$0.8 mm in diameter and 2–3 mm in length with polished (110), $(1\bar{1}1)$, and (001) faces. The BTO single crystal $x=0$ was obtained from MTI Corp. (Richmond, CA).

Raman spectra were recorded using a SPEX Triplemate spectrometer equipped with a liquid-nitrogen-cooled multichannel coupled-charge-device detector. The samples were attached to the cold finger inside a continuous He flow cryostat. Spectra were recorded in backscattering geometry in parallel $z(x,x)\bar{z}$ and perpendicular $z(x,y)\bar{z}$ polarization configurations. [z axis in most cases was parallel to the (110) direction of initial cubic phase, for $Ba_{0.5}Sr_{0.5}TiO_3$ crystal we measured the spectra along (001) direction, too.] The 514.5 nm Ar^+ laser line was used for excitation. The laser beam was focused to a spot of $\sim$300 μm diameter, and the laser power density was kept at a low level ($\leqslant$30 W/cm^2) to avoid sample heating.

III. RESULTS AND DISCUSSION

A. Raman spectra at $T=5$ K

Raman spectra of BST crystals measured at $T=5$ K for $x=0$ (STO), 0.05, 0.1, 0.2, 0.35, 0.5, and 1 (BTO) are presented in Fig. 1. The spectra of pure BTO and STO crystals are in agreement with those in the literature.[6,7,13–15] STO remains paraelectric down to low temperatures, and the zone-center optical phonons remain Raman inactive. The spectrum of STO crystal is dominated by the second-order features. Sharp peaks at 45, 144, and 444 cm^{-1} are of R modes, which are zone-edge (R point) phonons becoming Raman active because of the double folding of the Brillouin zone due to structural phase transition at 105 K.[14]

Addition of Ba to STO changes the low-temperature lattice dynamics significantly. For $x=0.05$ the crystal becomes ferroelectric at about 60 K and T_c increases with x. Consequently, the low temperature Raman spectra of the BST crystals are dominated by the first order peaks. Two distinct lines of the TO_1 phonons, the soft modes of A and E symmetries, are seen in the low-frequency range, their frequencies being 25 and 47 cm^{-1}, respectively, for $Ba_{0.05}Sr_{0.95}TiO_3$, and depending strongly on temperature and the composition of the crystals. The soft mode behavior will be considered in detail in the next section. Other, higher frequency phonons (hard modes) are also observed, whose frequencies change slowly with composition. The spectra shown in Fig. 1 were measured in the scattering geometry with parallel polarizations of incident and scattered light. We did not observe any dependence of the spectra on the polarization configuration, even for the spectra measured along the (001) direction of

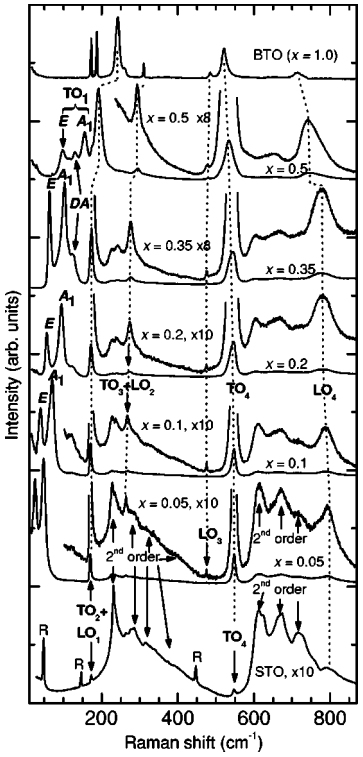

FIG. 1. Raman spectra of $Ba_xSr_{1-x}TiO_3$ crystals at 5 K. The spectra of pure $SrTiO_3$ and $BaTiO_3$ crystals are also shown. The peaks labeled *R* in the spectra of STO crystals are the structural modes. Vertical dashed-dotted lines are guides to the eye.

initial cubic phase. This is likely because our crystals were not poled during cooling down to low temperatures, and there are different domain orientations in the ferroelectric phases. Therefore the low temperature spectra of the crystals in both polarization configurations contain all the Raman active phonon modes.

The frequencies of observed phonon lines at 5 K for all compositions are given in Table I. The following phonon modes are present in the spectra of BST crystals of all (nonzero) Ba concentrations studied: the TO_1 soft mode (A_1 and E components), TO_2+LO_1, TO_3+LO_2, LO_3, TO_4, and LO_4 modes. Mode assignment is based on the literature data for pure STO and BTO crystals. It has been shown that in STO, the frequencies of TO_2 and LO_1 phonons nearly coincide,[15,16]

TABLE I. Frequencies (cm^{-1}) of observed lines in the Raman spectra of BST crystals of all compositions x at $T=5$ K. Arrows in the LO_1 column indicate that this mode was not distinguished from the TO_2 for all compositions except 0.5.

x	TO_1		LO_1	TO_2	TO_3 and LO_2	LO_3	TO_4	LO_4
	E	A_1						
0.05	25	47	→	170	264	475	548	789
0.1	40	70	→	171	268	475	547	787
0.2	56	94	→	172	274	475	544	780
0.35	66	104	→	173	276	473	542	778
0.5	97	155	174	191	294	476	535	747

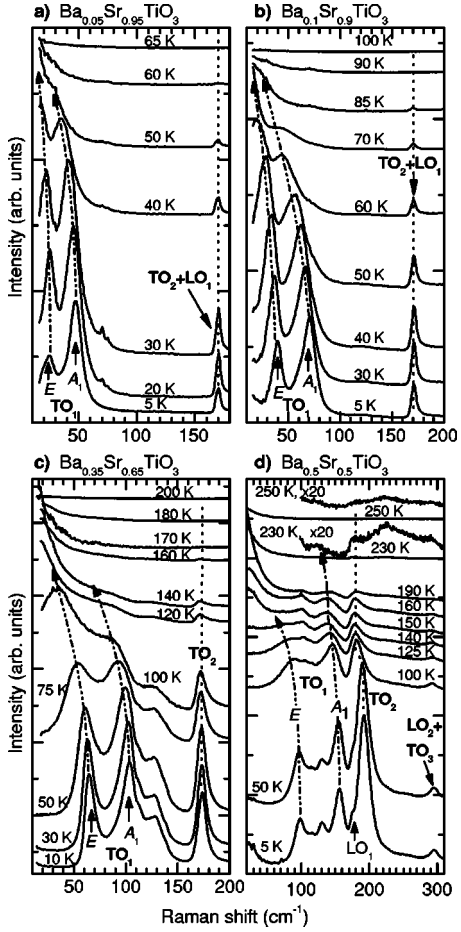

FIG. 2. Temperature evolution of low-frequency Raman spectra of $Ba_xSr_{1-x}TiO_3$ crystals with $x=0.05$, 0.1, 0.35, and 0.5 [(a)–(d), respectively]. Dashed-dotted lines indicate the soft modes.

whereas in pure BTO, the frequency of the TO_2 mode of A_1 symmetry is clearly higher than that of the LO_1 mode, and thus well separated.[11] In $Ba_{0.5}Sr_{0.5}TiO_3$ crystal, the shoulder on the low-frequency side of the TO_2 peak (more clearly seen in Fig. 2) is likely due to the LO_1 mode. The separation between these modes increases with x, and for $x \geqslant 0.5$ it becomes large enough to distinguish the modes in Raman spectra. Therefore, the Raman lines labeled as TO_2+LO_1 are assumed to contain contributions from both TO and LO modes. It has been shown that in STO[15,16] as well as in BTO,[8,11] the frequencies of TO_3 and LO_2 phonons also nearly coincide. Therefore, the Raman lines labeled as TO_3+LO_2 are also assumed to contain contributions from both TO and LO modes. The LO_4 phonon line is broad, which is probably due to an overlap with the second-order Raman features. This mode was observed at 795 cm^{-1} for pure STO by hyper-Raman scattering.[16]

It should be noted that in the spectra of $Ba_{0.05}Sr_{0.95}TiO_3$ crystal the structural *R* modes already disappeared, indicating that there is no antiferrodistortive phase transition for $x \geqslant 0.05$. This is consistent with the phase diagram for $Ba_xSr_{1-x}TiO_3$, reported by Lemanov *et al.*[18]

Several bands have been observed in the spectra of BST crystals in the frequency ranges 200–300 and

600–750 cm^{-1}. These broad bands are attributed to the second-order Raman scattering, similarly to the bands observed in pure STO.[14] In STO these second-order bands dominate the spectra in the entire temperature range. Their detailed assignment to various two-phonon processes in STO was made by Nilsen and Skinner.[14] In the BST crystals, the second-order lines appear at the similar positions (as can be seen in Fig. 1), but they have much weaker intensities compared to the first-order TO peaks in the ferroelectric phases. The temperature behavior of the second-order features is distinctly different from that of the first-order peaks. As it is discussed below, the first-order lines disappear in the paraelectric phase, while the second-order features remain in the spectra in the entire temperature range, including the cubic phase.

Another weak band at about 120–130 cm^{-1} (labeled *DA* in Fig. 1) is seen in the spectra of BST crystals, and its intensity increases with *x*. Lemanov mentioned an observation of this feature in Raman spectra of BST ceramics and attributed it to the first-order Raman scattering by non-zone-center phonons activated by alloy disorder.[34] This seems to be a reasonable explanation since this feature is not seen in pure STO, and its intensity increases with *x*, i.e., increased degree of alloying.

B. Temperature evolution of the soft phonon modes

Figure 2 shows the low-frequency Raman spectra (15–200 cm^{-1}) of $Ba_xSr_{1-x}TiO_3$ crystals with $x=0.05$, 0.1, 0.35, and 0.5 as a function of temperature. These spectra illustrate the following features in the temperature evolution of the phonon lines: (i) both *E* and A_1 components of the TO_1 mode clearly demonstrate softening with increasing temperature; (ii) the linewidth (damping) of the soft modes increases with temperature; (iii) in contrast to the TO_1 modes, the hard mode frequencies remain nearly unchanged over the entire temperature range of ferroelectric phases (this can be seen in Fig. 2 showing both the TO_1 and the TO_2 modes); (iv) the first-order Raman lines decrease in intensity as the temperature approaches the ferroelectric-paraelectric phase transition (T_c), and disappear completely above T_c.

The temperature dependence of the *E* and A_1 soft mode frequencies is shown in Fig. 3. The low-temperature soft mode frequencies are higher and the A_1-E splitting is larger for higher Ba content, indicating an increasing spontaneous polarization with *x*. According to the BST phase diagram of Lemanov *et al.*[18] obtained from the dielectric studies of BST ceramics, which is plotted in Fig. 4 by the dotted lines, all the data for the *E* mode presented in Fig. 3(a) correspond to the rhombohedral phase. The *E* mode frequency decreases with increasing temperature while its linewidth (damping) increases, and the peak of this mode becomes undistinguishable in the orthorhombic phase. The splitting of the double degenerated *E* mode of the rhombohedral phase into the B_1 and B_2 components in the orthorhombic phase were not observed. The A_1 mode frequency tends to zero when the temperature approaches T_c in BST crystals with $x \leqslant 0.2$, but shows much less softening for higher *x*. The square of the A_1 soft mode frequency is proportional to the spontaneous

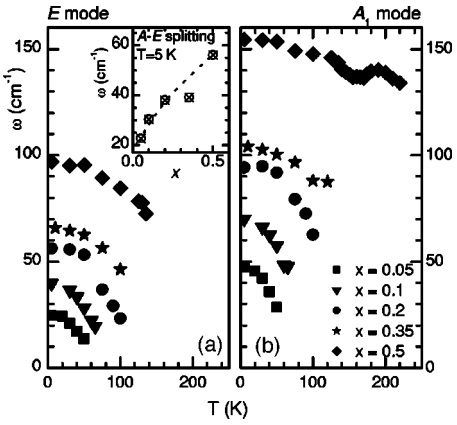

FIG. 3. Temperature dependence of the *E* and A_1 soft mode frequencies (left and right panels, respectively) for all compositions of BST crystals studied. Inset shows the composition dependence of the A_1-E mode splitting at 5 K.

polarization.[8,9] The fact that the A_1 mode frequency does not tend to zero at T_c is evidence that the polarization has discontinuity at this point. The ferroelectric phase transition is known to be of the first order for BTO, and it becomes of the second order for $x<0.2$. This is consistent with the results of dielectric studies of BST ceramics by Lemanov *et al.*[18] In the $Ba_{0.5}Sr_{0.5}TiO_3$ crystal the temperature dependence of the A_1 mode frequency undergoes small jump at ~175 K and inflection at ~145 K, indicating the tetragonal-orthorhombic and orthorhombic-rhombohedral phase transitions.

Our results of BST crystals show a dramatically reduced coupling in the tetragonal phase between the A_1 soft mode and the TO_2 hard mode of A_1 symmetry characteristic of the pure BTO.[8,44] In BTO, the two peaks merge into a broad band centered at about 250 cm^{-1} at T_c. The characteristic features of the A_1 phonon spectrum in BTO—the interference of the sharp TO_1 line with the broad TO_2 mode and the broad asymmetric TO_2 and TO_4 features—were interpreted by the coupling between these three modes of A_1 symmetry related to the disorder behavior.[8,44] Some indications of

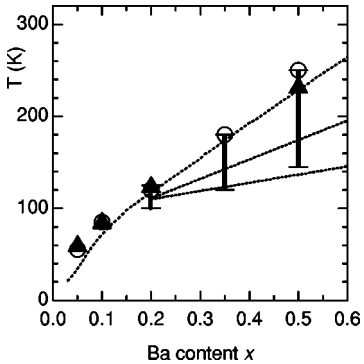

FIG. 4. The ranges of the intensive low-frequency scattering as a function of Ba contents *x* for $Ba_xSr_{1-x}TiO_3$ crystals (vertical bars). Open circles show the ferroelectric phase transition temperatures for crystals as determined from the intensities of the first-order Raman peaks. Triangles indicate the positions of peaks in the temperature dependence of the dielectric constant. Dotted lines represent the phase diagram for bulk BST (Ref. 18).

the A_1 mode coupling can be seen in the spectra of $Ba_{0.5}Sr_{0.5}TiO_3$ crystal, e.g., asymmetry of the TO_2 peak in the temperature range 100–225 K. However, the coupling is much less pronounced than in pure BTO, and there is no sharp interference dip between the TO_1 and TO_2 modes as in pure BTO. Further, as clearly seen in Fig. 2, the coupling decreases with decreasing Ba content. This is consistent with the results by Kuo *et al.*,[37] who also observed disappearance of the interference dips between the A_1 TO_1 and TO_2 modes in the Raman spectra of BST for Ba compositions $x<0.6$, which is in the cubic phase at room temperature and the Raman spectra are dominated by the second-order features. Our results demonstrate the same, as the BST crystals of all compositions studied in the present paper are paraelectric at room temperature and show no first-order Raman scattering.

In $Ba_xSr_{1-x}TiO_3$ of the compositions studied here the peaks of A_1 (TO_1) and A_1 (TO_2) modes remain distinctly separated in the entire temperature range below the ferroelectric-paraelectric phase transition, as shown in Fig. 2(d). The A_1 soft mode disappears at T_c, while the A_1 TO_2 mode merges with the second-order Raman line centered at ~ 225 cm^{-1} and then disappears as well. This behavior allows us to use the vanishing intensity of the A_1 soft mode to determine T_c, in particular in the case of a first-order phase transition when the polarization has a discontinuity at T_c, and the A_1 soft mode does not tend to the same frequency as E mode at the phase transition temperature. This approach is very useful for BST thin films where dielectric measurements do not always allow the determination of the phase transition temperature.[45] For BST crystals with low Ba content no signs of the A_1 mode coupling have been observed in the spectra.

Another difference in the soft mode behavior of BST crystals with different Ba contents is the E soft mode damping. In pure $BaTiO_3$ the soft mode is heavily overdamped at the temperatures near T_c,[7–9] and remains overdamped in tetragonal phase. In the orthorhombic phase of BTO, Laabidi *et al.*[20] showed that the soft mode is also heavily damped ($\Gamma/\omega>1$) in the entire temperature range of the orthorhombic phase, although the damping decreases with temperature, and below 253 K $\Gamma/\omega<\sqrt{2}$, which allows one to consider the mode to be underdamped. However, intensive low-frequency, near-excitation scattering persists in the Raman spectra of the orthorhombic phase, and disappears at the orthorhombic-rhombohedral phase transition.[20] We observed similar behavior in BST crystals of high Ba content ($x \geqslant 0.2$). The spectra of the BST crystals in the orthorhombic phase [e.g., Fig. 2(d) at the temperatures 150, 160 K] are similar to those presented by Laabidi *et al.* for orthorhombic BTO. Drastic increase of the low-frequency scattering at the transition from the rhombohedral to orthorhombic phase is clearly seen. [See Fig. 2(d), the spectra of $Ba_{0.5}Sr_{0.5}TiO_3$ crystals at 140 K (rhombohedral phase) and 150 K (orthorhombic phase), or Fig. 2(c) the spectra of $Ba_{0.35}Sr_{0.65}TiO_3$ crystals at 100 and 120 K.]

The low-frequency near-excitation scattering in BTO was related to the central peak, which is attributed to the relaxational motion of the off-center Ti ions.[25–27] Although our data do not allow us to distinguish the central peak from the damped soft mode, we believe that the intensive low-frequency Raman scattering in BST, similarly to BTO, includes the contribution of both heavily damped soft mode and relaxational motion.

Figure 4 shows the temperature ranges of the E mode overdamping for all compositions of BST crystals measured, in comparison with the phase diagram for BST.[18] (Here under the "range of overdamping" we mean the temperatures where the intensive low-frequency scattering was observed, and the soft mode is undistinguishable in the spectra.) As one can see, the intensive low-frequency scattering in BST crystals occurs mostly in the orthorhombic and tetragonal phases. The E soft mode is not overdamped in the rhombohedral phase, and it is not seen in the spectra above T_c, becoming Raman inactive in the cubic phase. (It should be noted that according to the phase diagram of BST obtained by Lemanov *et al.*[18] the temperature of 140 K corresponds to the orthorhombic phase for $x=0.5$, but the spectra of our crystal at this temperature indicate that the crystal is likely to be in rhombohedral phase.) As the temperatures of the three phase transitions converge with decreasing x, the range of overdamping narrows. Overdamping was not observed for BST crystals with $x=0.1$ and 0.05.

Since the three phase transitions in BTO and BST with $x \geqslant 0.2$ are related to the order-disorder effects, and the lowest-temperature phase is completely ordered, one can suggest that there will be no overdamping in the rhombohedral phase. For $x<0.2$, where only one ferroelectric phase exists, the displacive behavior should be dominant, and the soft mode is not overdamped as we have observed experimentally. The above mentioned fact that coupling of the A_1 modes in $Ba_{0.5}Sr_{0.5}TiO_3$ crystals is much less pronounced compared to pure $BaTiO_3$, and disappearance of the coupling for smaller x also indicates decreased degree of disorder for crystals with lower Ba content.

C. Hard modes: The composition and temperature dependences

In this section we consider the behavior of optical phonons other than the TO_1—the hard modes. Figure 5 shows the variation of the hard mode frequencies with Ba content x at $T=5$ K. Our data for the composition range studied complement the data reported by Lemanov[34] by presenting the mode assignment and making clear distinction between the first- and second-order Raman features, which were presented in the Ref. 34 together in the same graphs. Also, we add the data for the LO_3 phonon. This weak line presents the spectra of all BST compositions studied, as well as pure $BaTiO_3$. For STO, it was observed at 475 cm^{-1} by hyper-Raman scattering.[16]

Most hard modes exhibit a weak decrease of their frequencies with increasing temperature. The frequency shift is more noticeable in BST crystals with larger x, which remain in ferroelectric phase up to higher temperatures, making possible the observation of the phonon lines in Raman spectra over broader temperature range. Figure 6 shows the temperature dependence of the TO_2 and TO_4 phonon frequencies for all compositions studied. These two modes show the most

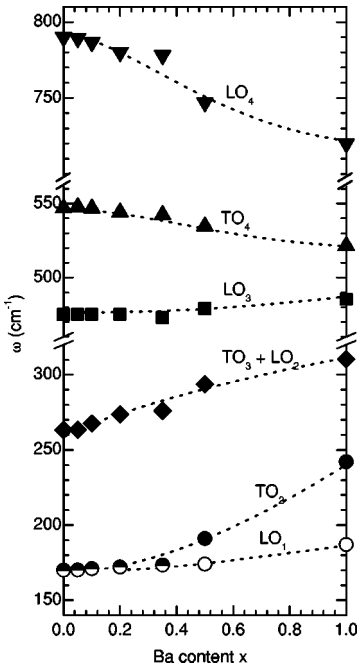

FIG. 5. Composition dependence of the hard phonon mode frequencies at 5 K. Dotted lines are guides to the eye. The half-solid circles label the TO_2 and LO_1 modes, undistinguishable in spectra.

significant changes with temperature. For all compositions except 0.5 the phonon frequencies decrease monotonously with increasing temperature. For $Ba_{0.5}Sr_{0.5}TiO_3$ crystals the TO_2 mode frequency decreases with increasing temperature up to about 140 K, then remains nearly constant up to 175 K, where it jumps up for about 2 cm^{-1}. This behavior correlates with that of the A_1 soft mode (Fig. 3), indicating the tetragonal-orthorhombic and orthorhombic-rhombohedral phase transitions. The pronounced jumps of the TO_2 mode frequency at these phase transitions are characteristic for $BaTiO_3$ crystals.[6,12,13]

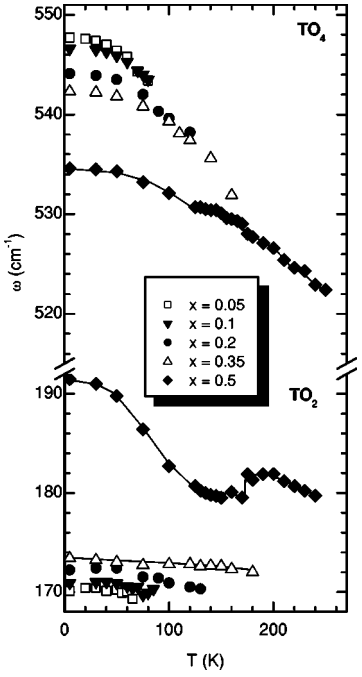

FIG. 6. Temperature dependence of the TO_2 and TO_4 phonon frequencies for $Ba_xSr_{1-x}TiO_3$ crystals.

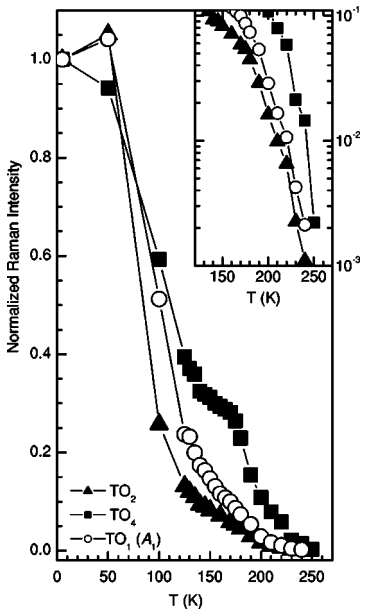

FIG. 7. Temperature dependence of relative Raman intensities of TO_2 and TO_4 phonons as well as the TO_1 (A_1 soft mode) for $Ba_{0.5}Sr_{0.5}TiO_3$ crystals. Each mode intensity is normalized by the Bose factor $n+1=(1-\exp(-\hbar\omega/kT))^{-1}$, and divided by the corresponding intensity at 5 K. Inset shows the enlarged part of the figure near the T_c (logarithmic scale).

Figure 7 shows the temperature dependence of the hard mode intensities. The A_1 TO_1 soft mode intensity is also shown. The intensities are normalized by the Bose factor $n+1=(1-\exp(-\hbar\omega/kT))^{-1}$, and divided by the intensity of the corresponding mode at 5 K. The A_1 soft mode exists in ferroelectric phases only. Its intensity decreases as the temperature approaches the T_c from below, and vanishes at T_c, as it was mentioned in the preceding section. The Raman intensities of the hard modes also decrease with increasing temperature and the phonon lines disappear above T_c, becoming Raman inactive due to the symmetry selection rules.

Again, the behavior of the TO_2 and TO_4 phonon modes in BST is different from that in pure $BaTiO_3$. In BTO, the broad features at 260 and 530 cm^{-1} are observed,[8,46] and assigned to the TO modes, having A_1 symmetry in tetragonal phase and remaining in the spectra upon the transition into the cubic phase.[8] More recent studies reported the temperature evolution of the Raman spectra of BTO in tetragonal and cubic phases,[47,48] have clearly demonstrated that these features are due to the first-order Raman scattering by TO phonons, which persist in the spectra up to the temperatures well above the tetragonal-cubic phase transition in BTO. The breakdown of the Raman selection rules was attributed to the order-disorder behavior—the off-center motion of Ti ions locally breaking the inversion symmetry.[8,48] The absence of the first-order Raman lines in the spectra of cubic phase of $Ba_xSr_{1-x}TiO_3$ with $x \leqslant 0.5$ studied here, indicates that BST has a significantly lower degree of disorder compared to BTO.

The fact that the selection rules are obeyed in BST allows one to determine the T_c from the temperature dependence of Raman intensities. As one can see from Fig. 7, the intensities of both hard modes and the A_1 soft mode vanish at the same temperature. Similar behavior was observed for BST crystals of all compositions studied.

It should be noted that in thin films the symmetry selection rules are not strictly obeyed because of defects, and weak features of the hard modes are seen in Raman spectra even in the cubic phase.[39] This makes it more difficult to use Raman intensity of the hard modes to determine T_c. But the A_1 soft mode still can be used if the phase transition is of the first order, as it was discussed in Sec. III B. In this case the polarization has a discontinuity at T_c, and the A_1 mode appears in the ferroelectric phase at a frequency, at which no phonon mode exists in the cubic phase.

IV. SUMMARY

We have studied the phonon properties of $Ba_xSr_{1-x}TiO_3$ single crystals with $x=0.05$, 0.1, 0.2, 0.35 and 0.5 by Raman spectroscopy in the temperature range 5–300 K. At low temperatures two components of the TO_1 soft phonon, the E and A_1 modes have been observed for all compositions studied. Heavy damping of the soft mode and the intensive low-frequency Raman scattering related to the order-disorder behavior are observed in BST crystals with $x \geqslant 0.2$ in the temperature and composition diapason of the orthorhombic and tetragonal phases. There is no soft mode overdamping in the rhombohedral phase, which is completely ordered, and the soft mode is Raman inactive in the cubic phase of BST. The behavior characteristic for the order-disorder phase transitions becomes less noticeable with decreasing Ba content. $Ba_xSr_{1-x}TiO_3$ with $x \leqslant 0.2$ can be considered as predominantly displacive type ferroelectrics with single ferroelectric phase and well-defined soft mode in the entire temperature range. The composition and temperature dependencies of the hard phonon modes shows that other features of the disorder behavior characteristic for pure $BaTiO_3$, such as the coupling of the TO modes of the A_1 symmetry and the presence of the first-order Raman peaks in the cubic phase, are much less pronounced in BST. The weak indications of the A_1 mode coupling were observed for $Ba_{0.5}Sr_{0.5}TiO_3$ crystals only, and the first-order scattering in the paraelectric phase was not observed in the BST crystals of all the compositions studied.

The TO_1 A_1 soft mode frequency decreases significantly and tends to merge with the E mode when temperature approaches T_c from below in BST crystals with $x \leqslant 0.2$, but the A_1 mode shows much less softening in crystals with higher Ba content. This indicates that the polarization is discontinuous at T_c in crystals with $x > 0.2$, but the discontinuity apparently disappears for smaller x, i.e., the ferroelectric phase transition known to be of the first order for pure $BaTiO_3$, is also of the first order in $Ba_xSr_{1-x}TiO_3$ with high Ba content, but turns into the second order for $x < 0.2$.

ACKNOWLEDGMENTS

This work was partially supported by DOE under Grant No. DE-FG02-01ER45907, by DARPA under Grant No. DABT63-98-1-002, and by NSF under Grant No. DMR-0103354.

*Electronic address: dat10@psu.edu

[1] F. Jona and G. Shirane, *Ferroelectric Crystals* (Dover, New York, 1993).
[2] M. E. Lines and A. M. Glass, *Principles and Applications of Ferroelectrics and Related Materials* (Oxford University Press, New York, 1977).
[3] *Thin Film Ferroelectric Materials and Devices*, edited by R. Ramesh (Kluwer Academic, Boston, 1997).
[4] *Ferroelectric Thin Films: Synthesis and Basic Properties*, edited by C. P. de Araujo, J. F. Scott, and G. W. Taylor (Gordon and Breach, Amsterdam, 1996).
[5] W. Cochran, Adv. Phys. **9**, 387 (1960).
[6] C. H. Perry and D. B. Hall, Phys. Rev. Lett. **15**, 700 (1965).
[7] M. DiDomenico, Jr., S. P. S. Porto, and S. H. Wemple, Phys. Rev. Lett. **19**, 855 (1967); M. DiDomenico, Jr., S. H. Wemple, S. P. S. Porto, and R. P. Bauman, Phys. Rev. **174**, 522 (1968).
[8] A. Scalabrin, A. S. Chaves, D. S. Shim, and S. P. S. Porto, Phys. Status Solidi B **79**, 731 (1977).
[9] G. Burns and F. H. Dacol, Phys. Rev. B **18**, 5750 (1978).
[10] H. Vogt, J. A. Sanjurjo, and G. Rossbroich, Phys. Rev. B **26**, 5904 (1982); H. Presting, J. A. Sanjurjo, and H. Vogt, *ibid.* **28**, 6097 (1983).
[11] J. D. Freire and R. S. Katiyar, Phys. Rev. B **37**, 2074 (1988).
[12] U. D. Venkateswaran, V. M. Naik, and R. Naik, Phys. Rev. B **58**, 14256 (1998).
[13] M. Osada, M. Kakihana, S. Wada, T. Noma, and W.-S. Cho, Appl. Phys. Lett. **75**, 3393 (1999).
[14] W. G. Nilsen and J. G. Skinner, J. Chem. Phys. **48**, 2240 (1968).
[15] P. A. Fleury and J. M. Worlock, Phys. Rev. **174**, 613 (1968).
[16] H. Vogt and G. Rossbroich, Phys. Rev. B **24**, 3086 (1981); H. Vogt, *ibid.* **38**, 5699 (1988).
[17] *Landolt-Börnstein Numerical Data and Functional Relationships in Science and Technology*, New Series, Group III, Vol. 16 (Springer, New York, 1981), p. 67.
[18] V. V. Lemanov, E. P. Smirnova, P. P. Syrnikov, and E. A. Tarakanov, Phys. Rev. B **54**, 3151 (1996).
[19] K. A. Müller and H. Burkard, Phys. Rev. B **19**, 3593 (1979).
[20] K. Laabidi, M. D. Fontana, and B. Jannot, Solid State Commun. **76**, 765 (1990).
[21] J. Harada, J. D. Axe, and G. Shirane, Phys. Rev. B **4**, 155 (1971).
[22] R. Comes, M. Lambert, and A. Guinier, Solid State Commun. **6**, 715 (1968); Acta Crystallogr., Sect. A: Cryst. Phys., Diffr., Theor. Gen. Crystallogr. **26**, 244 (1970).
[23] K. A. Müller and W. Berlinger, Phys. Rev. B **34**, 6130 (1986).
[24] R. E. Cohen and H. Krakauer, Phys. Rev. B **42**, 6416 (1990).
[25] J. P. Sokoloff, L. L. Chase, and D. Rytz, Phys. Rev. B **38**, 597 (1988); **40**, 788 (1989).
[26] M. D. Fontana, K. Laabidi, and B. Jannot, J. Phys.: Condens.

Matter **6**, 8923 (1994).
[27] T. P. Dougherty, G. P. Wiederrecht, K. A. Nelson, M. H. Garrett, H. P. Jenssen, and C. Warde, Phys. Rev. B **50**, 8996 (1994).
[28] B. Zalar, V. V. Laguta, and R. Blinc, Phys. Rev. Lett. **90**, 037601 (2003).
[29] M. Stachiotti, A. Dobry, R. Migoni, and A. Bussmann-Holder, Phys. Rev. B **47**, 2473 (1993).
[30] A. Bussmann-Holder, J. Phys. Chem. Solids **57**, 1445 (1996).
[31] Y. Girshberg and Y. Yakobi, J. Phys.: Condens. Matter **11**, 9807 (1999).
[32] H. J. Bakker, Phys. Rev. B **52**, 4093 (1995).
[33] W. Zhong, D. Vanderbilt, and K. M. Rabe, Phys. Rev. Lett. **73**, 1861 (1994); Phys. Rev. B **52**, 6301 (1995).
[34] V. V. Lemanov, Phys. Solid State **39**, 318 (1997).
[35] P. S. Dobal, A. Dixit, R. S. Katiyar, D. Garcia, R. Guo, and A. S. Bhalla, J. Raman Spectrosc. **32**, 147 (2001).
[36] R. Naik, J. J. Nazarko, C. S. Flattery, U. D. Venkateswaran, V. M. Naik, M. S. Mohammed, G. W. Auner, J. V. Mantese, N. W. Schubring, A. L. Micheli, and A. B. Catalan, Phys. Rev. B **61**, 11 367 (2000).
[37] S.-Y. Kuo, W.-Y. Liao, and W.-F. Hsieh, Phys. Rev. B **64**, 224103 (2001).
[38] D. A. Tenne, A. M. Clark, A. R. James, K. Chen, and X. X. Xi, Appl. Phys. Lett. **79**, 3836 (2001).
[39] D. A. Tenne, A. Soukiassian, M. H. Zhu, A. M. Clark, X. X. Xi, H. Choosuwan, Qi He, R. Guo, and A. S. Bhalla, Phys. Rev. B **67**, 012302 (2003).
[40] J. Petzelt and T. Ostapchuk, Ferroelectrics **267**, 93 (2002).
[41] Yu. I. Yuzyuk, V. A. Alyoshin, I. N. Zakharchenko, E. V. Sviridov, A. Almeida, and M. R. Chaves, Phys. Rev. B **65**, 134107 (2002); Yu. I. Yuzyuk, P. Simon, I. N. Zakharchenko, V. A. Alyoshin, and E. V. Sviridov, *ibid.* **66**, 052103 (2002); Yu. I. Yuzyuk, J. L. Sauvajol, P. Simon, V. L. Lorman, V. A. Alyoshin, I. N. Zakharchenko, and E. V. Sviridov, J. Appl. Phys. **93**, 9930 (2003); Yu. I. Yuzyuk, R. S. Katiyar, V. A. Alyoshin, I. N. Zakharchenko, D. A. Markov, and E. V. Sviridov, Phys. Rev. B **68**, 104104 (2003).
[42] T.-G. Kim, J. Oh, T. Moon, Y. Kim, B. Park, Y.-T. Lee, and S. Nam, J. Mater. Res. **18**, 682 (2003).
[43] D. Garcia, R. Guo, and A. S. Bhalla, Integr. Ferroelectr. **42**, 57 (2002).
[44] A. S. Chaves, R. S. Katiyar, and S. P. S. Porto, Phys. Rev. B **10**, 3522 (1974).
[45] O. G. Vendik and S. P. Zubko, J. Appl. Phys. **88**, 5343 (2000).
[46] M. P. Fontana and M. Lambert, Solid State Commun. **10**, 1 (1972).
[47] S. Wada, T. Suzuki, M. Osada, M. Kakihana, and T. Naoma, Jpn. J. Appl. Phys., Part 1 **37**, 5385 (1998).
[48] Y.-J. Jiang, L.-Z. Zeng, R.-P. Wang, Y. Zhu, and Y.-L. Liu, J. Raman Spectrosc. **27**, 31 (1996); L. M. Li, Y.-J. Jiang, and L.-Z. Zeng, *ibid.* **27**, 503 (1996).